2020 IEEE Intelligent Vehicles Symposium (IV)
October 20-23, 2020. Las Vegas, USA

Towards Synchronisation of Multiple Independent MEMS-based Micro-Scanning LiDAR Systems

Philipp Stelzer[1], Andreas Strasser[1], Christian Steger[1], Hannes Plank[2] and Norbert Druml[2]

***Abstract*— In intelligent vehicles, it is indispensable to have reliable Advanced Driver-Assistance Systems (ADAS) on board. These ADAS require various types of sensors, like Light Detection and Ranging (LiDAR). Nowadays, drivers delegate some responsibilities to their highly automated vehicles; however, it is not legally secured. Nevertheless, the legislator will, in the future, deal with automated vehicles. The fundamentals will be laid to ensure that the transfer of responsibilities will be permitted under certain conditions. Car manufacturers, on the other hand, must ensure that components are safe and reliable. With LiDAR, this could be achieved with Micro-Electro-Mechanical System (MEMS) technology. As with humans as drivers, it is also advantageous for intelligent systems if obstacles in the environment are detected promptly. Especially when the obstacles are moving, it helps to initiate appropriate measures, such as braking. Therefore, it is attempted to extend the Field-of-View (FoV) of the various sensors. By synchronising multiple MEMS mirrors, it is able to extend the FoV of the LiDAR part in an environmental perception system. In this publication, an architecture is proposed for MEMS-based Micro-Scanning LiDAR Systems to achieve synchronisation of multiple independently controlled MEMS mirrors. The architecture was implemented in an FPGA prototyping platform to show its feasibility and evaluate its performance.**

I. Introduction

In the present, but of course in the future, not all of the traffic participants are able to communicate with each other [1]. Pedestrians, for example, are not always able to communicate their intentions to drivers, and in the future, perhaps only to cars. A communication between pedestrians and vehicles could be done over 5G or another transmission standard [2], [3]. A major disadvantage, however, is that the pedestrian has to carry a mobile phone or other communication devices with him in any case. This leads us to the problem that, for example, children playing in a residential street cannot communicate with the highly automated vehicle without a mobile phone. Therefore, in addition to communication with the infrastructure and other traffic participants, it is absolutely necessary to also perceive the surroundings via cameras, radio detection and ranging (RADAR) and of course light detection and ranging (LiDAR) sensors. This is the aim of the PRogrammable sYSTems for INtelligence in automobilEs (PRYSTINE) project. PRYSTINE is aiming a Fail-operational Urban Surround perceptION (FUSION) on the basis of robust RADAR and LiDAR fusion [4]. In Figure 1 is illustrated how the intended FUSION should look like, in order to enable safe automated driving in urban and rural areas. What vehicles must meet in order to be declared as automated is defined in a standard published by the Society of Automotive Engineers (SAE) [5]. For example, the requirements for Advanced Driver-Assistance Systems (ADAS) are defined in that standard, so that fully automated driving is possible at all. How such architectures could look like for an environmental perception system is explained by Kohn et al. [6]. Therefore, it is important that automotive qualified RADAR and LiDAR components become affordable to be installed in large car fleets for environmental perception. Yoo et al. [7] have presented an automotive qualified MEMS-based LiDAR, which can be a key enabler for affordable LiDAR sensor systems in highly automated vehicles. However, in order to achieve the largest possible Field-of-View (FoV), multiple independent MEMS-based LiDAR systems must be used in synchronisation. These must be synchronised, because in asynchronous, independently controlled LiDAR systems, this can lead to interferences in the receiver modules of the individual LiDAR systems. These interferences can cause ghost objects to be detected, for example [8]. Hence, this paper is dealing with a synchronisation of multiple independently controlled MEMS mirrors. Thus, with our paper contribution we:

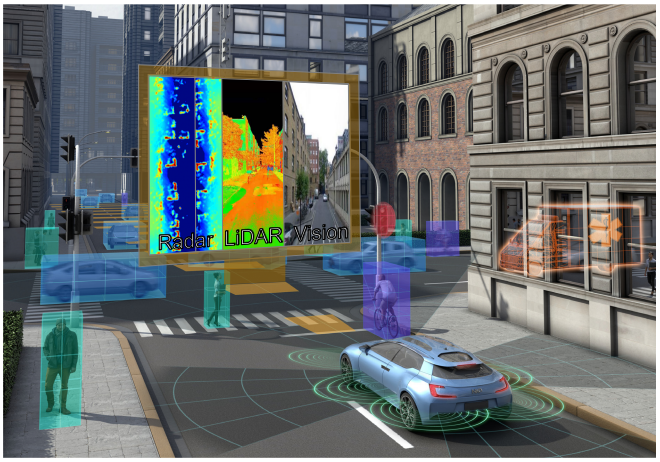

Fig. 1. PRYSTINE's concept view of a Fail-operational Urban Surround perceptION (FUSION) [4].

- achieve a synchronisation of multiple independent MEMS-based LiDAR systems,
- include a larger FoV due to multiple LiDARs and
- enhance safety due to the wider and deeper FoV.

The remainder of the paper is structured as follows. The overview of related work of MEMS-based LiDAR systems and other non-linear systems, which are synchronised, is

[1]Institute of Technical Informatics, Graz University of Technology, 8010 Graz, Austria {stelzer, strasser, steger}@tugraz.at
[2]ATV Sense and Control, Infineon Technologies Austria AG, 8020 Graz, Austria {hannes.plank, norbert.druml}@infineon.com

given in Section II. The novel synchronisation procedure of MEMS-based LiDAR systems will be presented in detail in Section III, and the achieved results, including a short discussion, will be provided in Section IV. A summary and short discussion of the findings will conclude this paper in Section V.

II. Related Work

Currently, there are already LiDAR systems available, such as the Velodyne HDL-64E [9], that cover a large FoV. However, the disadvantages of such LiDARs outweigh the advantages. On the one hand, they are very cost intensive and, on the other hand very bulky. Thus, academia and industry are researching for a low cost, long-range, and automotive qualified LiDAR solution. Druml et al. [10] have introduced a MEMS-based LiDAR system, which is cost effective, robust, automotive qualified, and long-range capable. Due to the fact that Druml et al.'s system has either a small and long-range FoV or a wide and short-range FoV, it is necessary to consider a way to achieve both.

A. 1D MEMS Micro-Scanning LiDAR

The 1D micro-scanning LiDAR approach, which is pursued by Druml et al., typically deflects a vertical laser beam line into the scenery and performs a horizontal scanning. In Figure 2, this functional principle is shown. How the field of view can be changed is explained in the following. At first, Druml et al.'s system is introduced to gain a comprehension of the properties responsible for the different FoV sizes of MEMS-based LiDARs. An ordinary MEMS-based LiDAR is composed of an Emitter path, a Receiver path, and a System Safety Controller (AURIX) [11] that coordinates Emitter path and Receiver path as depicted in Figure 3. Basically, the MEMS mirror's frequency is indirectly responsible for the size and depth of the obtained FoV. Therefore, we have concentrated on the Emitter path, especially on the MEMS Driver ASIC, of Druml et al.'s LiDAR system. The MEMS Driver deals with actuating, sensing, and controlling the MEMS mirror. According to Borovic et al. [12], a MEMS device can be operated either in an open-loop or closed-loop. The MEMS-based LiDAR system is commonly operated in a closed-loop mode to ensure a robust scan shape. The maximum deflection angle is derived from the configured frequency of the MEMS mirror, which is operated in a

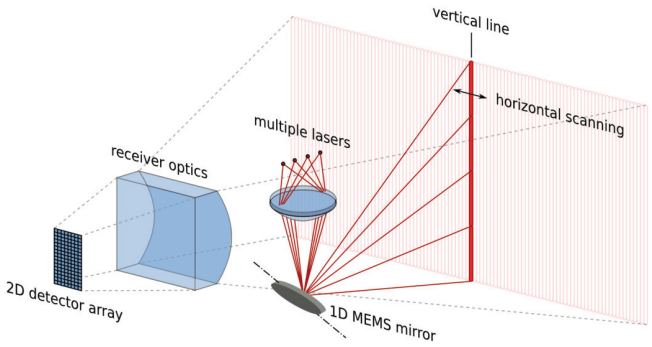

Fig. 2. Functional principle of a 1D micro-scanning LiDAR [10].

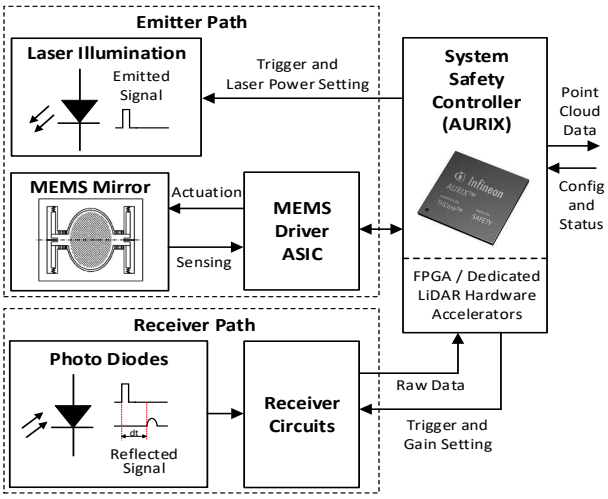

Fig. 3. System concept of a 1D MEMS-based automotive LiDAR system by Druml et al. [10].

closed-loop mode. Thus, the MEMS Driver is implicitly responsible for the maximum deflection angle of the MEMS mirror, since the actuation frequency is set there. The MEMS mirror is actuated by switching a High Voltage (HV) on and off. During the HV on phases, the mirror is pulled towards zero position. Switching off the HV causes the mirror to oscillate towards its maximum deflection. Stelzer et al. [13] have shown that the maximum deflection angle is derived from the actuation frequency. A low MEMS mirror oscillation frequency causes a narrow but long-range FoV and a higher MEMS mirror oscillation frequency causes a wider but shorter range FoV. The frequency of the MEMS mirror can be determined, e.g., by means of the position information. For accurate position information of the MEMS mirror, the MEMS Driver provides crucial signals. These are, among others, the POSITION_L and DIRECTION_L signals. A logical high POSITION_L signal represents a MEMS mirror alignment to the left and otherwise to the right. The DIRECTION_L signal on logical high represents a movement to the left and otherwise to the right. Both signals are set by an internal schedule.

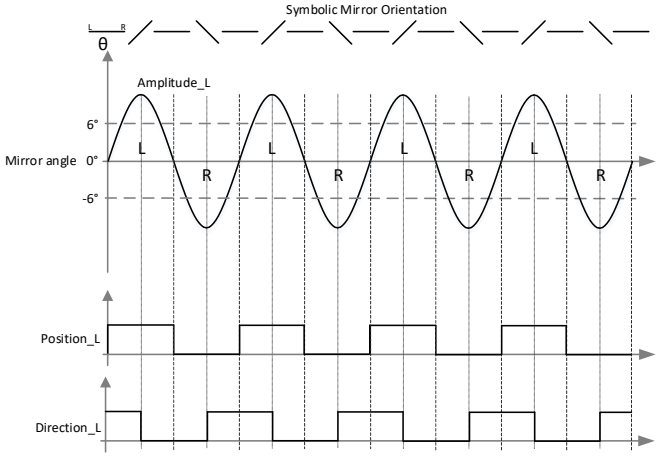

Fig. 4. Crucial signals of a MEMS mirror in a MEMS-based micro-scanning LiDAR system.

B. Non-linear Systems in Synchronisation

One way to extend the FoV of MEMS-based LiDARs would be the synchronisation of multiple independently controlled MEMS mirrors. Strasser et al. [14], e.g., have presented an approach for synchronising multiple MEMS mirrors. But this approach has a significant drawback. When operating the MEMS mirror with the control strategy of a phased-locked loop (PLL) [15], there is usually an internal reference signal for the feedback loop. With the approach presented by Strasser et al., however, the internal reference signal of the Slave is replaced by the Zero Crossing (ZC) signal of the Master. Consequently, there is no longer a closed feedback loop in the Slave system. This can lead to a worst-case scenario in which the actual Slave MEMS mirror's position no longer matches the position assumed by the Slave's MEMS Driver. Such a worst-case scenario can be caused, for example, by a huge unintended shock [16]. Then, if a wrong position is forwarded to the System Safety Controller, it would be fatal. The environmental perception system would then expect objects/obstacles at wrong positions. Furthermore, a simple synchronisation by setting the same HV(On/Off) values is not possible due to process variations. The same HV(On/Off) values most probably result in different mirror frequencies.

This raises a number of research questions:

- Is it possible to extend the FoV by synchronising multiple independently controlled MEMS mirrors while ensuring robust operation?
- Is it necessary to build the architectures of Master and Slave systems differently, or do extensions just have to be made so that they can be operated in both modes?

III. Novel Synchronisation Procedure

This section introduces the new synchronisation procedure that ensures robust and reliable operation of the entire LiDAR part of an environmental perception system. In Figure 5 is depicted how such a field of view could look like when synchronising multiple independently controlled MEMS mirrors. The FoV of the individual LiDAR systems is narrower but long-range. Synchronisation enables a long-range, narrow FoV of the individual LiDARs, so that the entire system has a long-range and wide FoV.

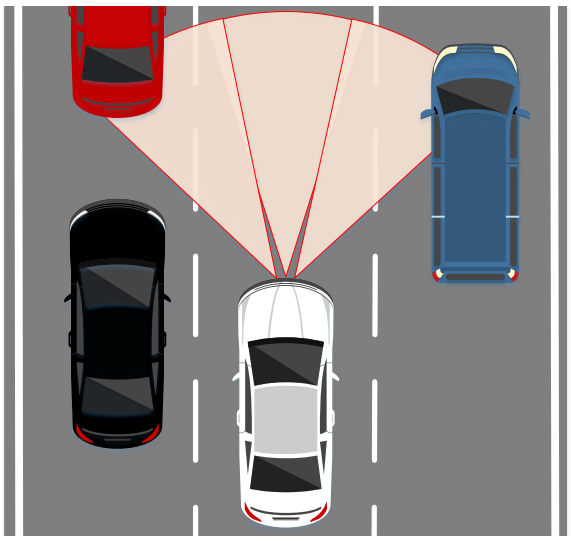

Fig. 5. Icon of multiple independently controlled and synchronised MEMS-based LiDAR systems, which are perceiving the environment together.

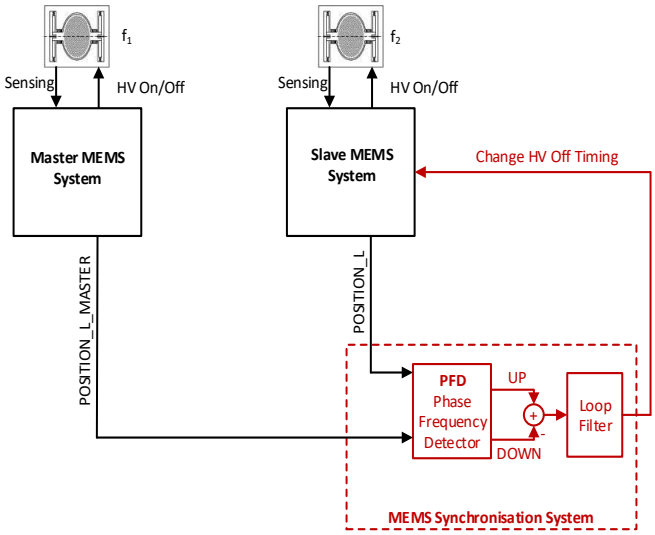

Fig. 6. Concept of a LiDAR system with two independently controlled MEMS mirrors in synchronistaion.

In Figure 6 is the fundamental synchronistaion concept with a Master MEMS system and one Slave MEMS system depicted. A Master MEMS system transmits the frequency of the Master MEMS mirror to at least one Slave MEMS system via the POSITION_L_MASTER signal. The respective POSITION_L signals of the slaves are then compared with the POSITION_L_MASTER signal. Adjustments are then made in the slaves accordingly. The architecture of a Slave MEMS system is explained below.

A. Slave Architecture for Synchronisation

This subsection describes the architecture of the Slave MEMS system. Such a system architecture of a slave is shown in Figure 7. In principle, any architecture, whether operated as Slave or Master, can be adapted for synchronous mode. It is possible to enable and disable the slave mode via the Slave Mode Enable (SMen) signal. When the slave mode is disabled, it can be operated as Master without any restrictions. The PLL architecture consists of a Phase Error Detector (PD), which outputs the mismatch of the actually measured Zero Crossing Measured (ZCmeas) signal and the internal Zero Crossing Reference (ZCref) signal in the form of an error value p(n). A loop filter, typically a PI controller, then uses this p(n) to calculate the new increment value of the subsequent Digitally Controlled Oscillator (DCO). With the frequency the DCO receives from the new increment DCO value, the internal schedule will be run faster or slower. The internal schedule in the Mirror Subtiming Block is the core of the MEMS Driver. Here, it is defined at which points in time measurements, processing and actuation are performed. The values set in HV(On/Off) determine at which times the HV is switched on and off. By varying these values, preferably

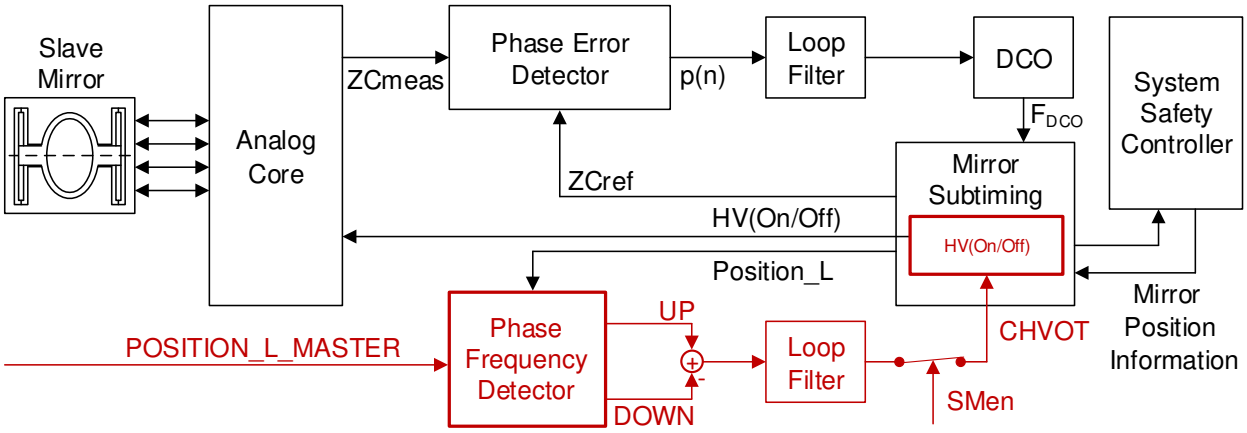

Fig. 7. Block diagram of the FPGA implementation of a Slave PLL architecture with additional blocks for synchronisation.

the HV Off value, the frequency of the MEMS mirror is influenced. A higher HV Off value, i.e., later switch-off time, results in a lower frequency of the MEMS mirror. A lower HV Off value corresponds to a higher MEMS mirror frequency. This brings us to our additions: The most important component we are adding is the Phase Frequency Detector (PFD). The PFD receives the POSITION_L signal and the external POSITION_L_MASTER signal as inputs. These are compared, similar to the PD. It is important that the frequency and phase are checked. Otherwise, it could cause the MEMS mirrors to have the same frequency but opposite phase. This counter value from the PFD is then forwarded to a loop filter, in our case a PI controller. Using appropriate controller parameters, the adjusted Counter HV Off Timing (CHVOT) value is then calculated. This CHVOT will replace the HV Off value in the Mirror Subtiming Block.

B. Synchronisation Procedure

Next, the synchronisation procedure is described in detail in this subsection. How the synchronisation procedure looks like is shown in Figure 8 and described in the following steps:

1) **Enabling Synchronous Mode**
   In the beginning, it is constantly checked in the background by software whether the synchronous mode is enabled or not. If the synchronous mode is then enabled, the slave mode must be enabled on the slave system(s). This can be done by the Master or the System Safety Control. The slave mode is enabled by the SMen switch.
2) **Configure Slave Init State**
   An initial HV Off Counter value is then set without calculation when the Slave mode starts. This value is the last used HV Off Counter value when synchronising to a Master MEMS mirror. This is used to speed up the synchronisation process at the same or similar frequencies.
3) **Enabling Phase Frequency Detector**
   Next, the PFD is enabled to compare the position signals of Slave and Master. As with the PD, there is also a time window in which the two position signals are compared. The counter value that is accumulated in this time window is then the error between Master and Slave. This error value is forwarded to the PI controller.

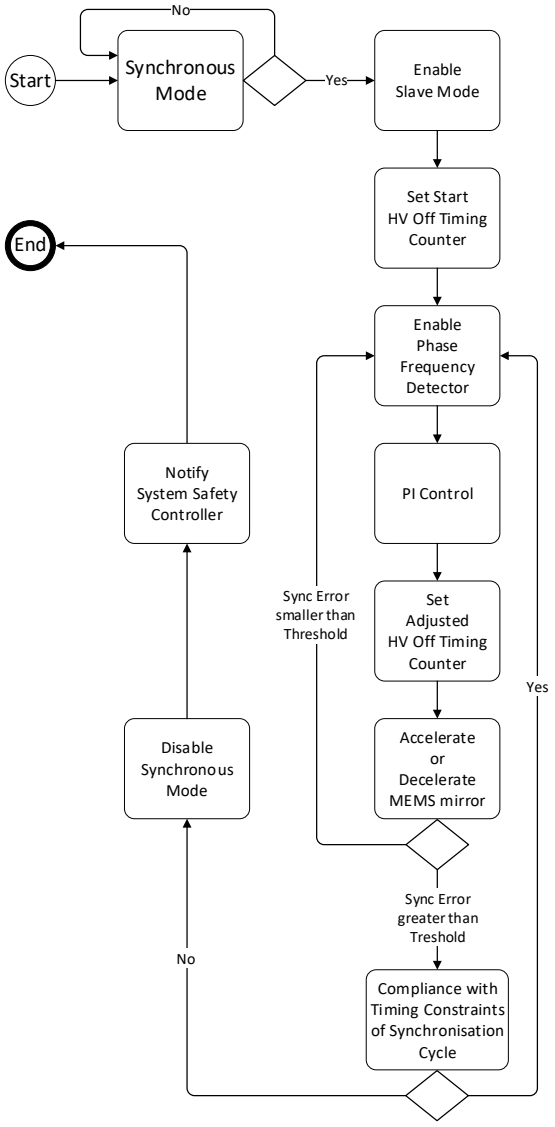

Fig. 8. Process flow of the Synchronisation Procedure from the Slave.

The counter is reset afterwards, and the counting is restarted in the next time window for the PFD.

4) **PI Control**
The forwarded error is used to calculate the new HV Off value. The calculated HV Off value is now CHVOT. This CHVOT is forwarded to the Mirror Subtiming Block. There it replaces the current HV Off value in the HV(On/Off) part with the new HV Off value.

5) **Check Synchronisation Error**
By adjusting the HV Off value, the frequency of the Slave MEMS mirror changes and outputs a changed position accordingly. The synchronisation error indicates how many clock cycles the position signals of Master and Slave are shifted.

a) **Synchronisation Success**
The synchronisation procedure is repeated periodically, as a frequency and phase change could occur respectively it is checked frequently whether the Slave MEMS mirror is still in synchronisation with the Master MEMS mirror. After a couple of adjustment cycles, the synchronisation error should be below a specific threshold value. If this is not the case, it is checked whether the timing constraints comply.

b) **Synchronisation Abort**
When these timing constraints are not met, the synchronisation process is aborted, and the slave mode is switched off by disabling SMen. In contrast to successful synchronisation, however, notification of failure is transmitted to the System Safety Controller. The System Safety Controller is then responsible for what measures are taken. Such measures could possibly be another attempt of synchronisation or degradation of the system.

With this new synchronisation procedure, it is now possible to create an enlarged field of view with multiple MEMS-based LiDAR systems. This significantly increases the safety and reliability of the overall environmental perception system, because no longer just a single LiDAR system does the LiDAR part of the overall environmental perception system.

IV. Results

In this section we provide the test results of our novel synchronisation procedure, which has been introduced in Section III. Our architecture was implemented in an FPGA Prototyping Platform by Yoo et al. [7]. This FPGA Prototyping Platform consists of a MEMS Driver Digital Part (FPGA), a MEMS Driver Discrete Analog Part, and the 1D MEMS mirror. For our test setup, we have used two of those FPGA Prototyping Platforms. One was operated as Master and the other as Slave. The POSITION_L_MASTER signal from the Master platform was provided to the synchronisation system in the Slave platform. During testing, the position signals of Master and Slave were measured with an oscilloscope. This was done in order to visually follow the synchronisation between the Master MEMS mirror and

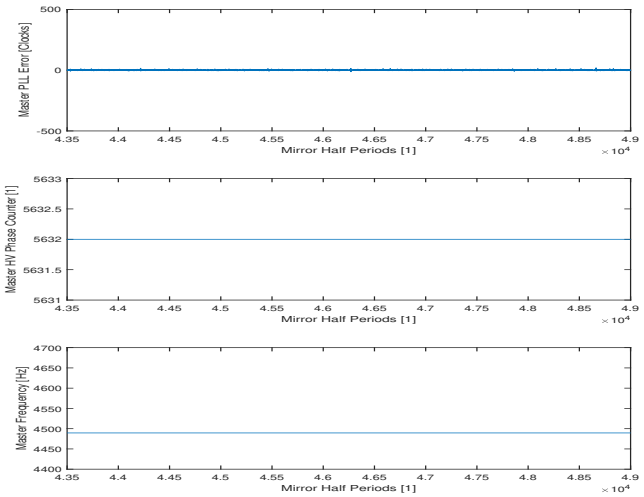

Fig. 9. Measurement during Master mirror's actuation with 4489 Hz.

the Slave MEMS mirror. Figure 11 shows the oscilloscope output before synchronisation and in synchronisation. Other essential parameters such as PLL errors, HV counter values, and frequencies of the individual systems, as well as the Synchronisation Error, were read out during periodic interrupts and sent to a PC for evaluation. The evaluated measurements will be discussed in the following. Figure 9 shows a measurement of the Master at 4489 Hz. It can be seen from the three measured parameters that the mirror operates smoothly and without any interference. That the frequencies of the MEMS mirror and the MEMS Driver match is shown by a constant low PLL error. A constant Master HV Phase Counter indirectly indicates that there are no frequency changes. This can be seen directly in the Master Frequency plot that the frequency is a constant 4489 Hz. Figure 10, shows the measurement of the Slave. In the beginning, it can be seen that the frequency is constant, and the MEMS mirror is operated smoothly and without interference, just like the Master. Only the Synchronisation Error oscillates between the maximum error limits. This is also evident because the two mirrors are operated at

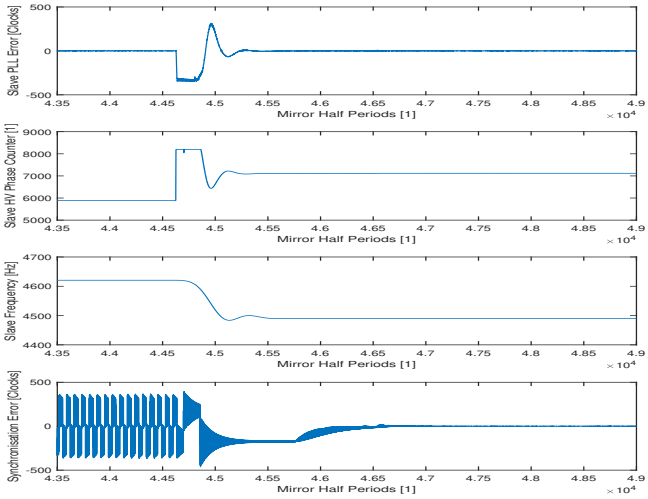

Fig. 10. Measurement, while the Slave MEMS mirror is operated in asynchronous and subsequently in synchronous mode.

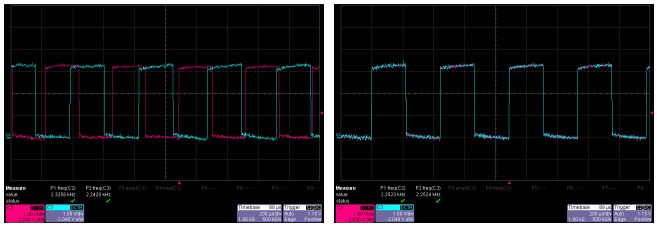

Fig. 11. Asynchronous (left) and synchronous (right) position signals of the Master and the Slave.

different frequencies. When switching to synchronous mode, significant changes in PLL Error, Slave HV Phase Counter, and Slave Frequency are detected. First, the Slave HV Phase Counter is changed significantly to reach the desired frequency faster. After that the Slave HV Phase Counter value will slowly settle down. By changing the Slave HV Phase Counter the frequency changes accordingly. The PLL Error is caused by a mismatch between the MEMS mirror and MEMS Driver during the adjustment phase. After the adjustment phase, the PLL Error also settles down. Table I shows the results of the synchronisation procedure. It takes about 110 ms until the Slave MEMS mirror reaches the frequency of the Master MEMS mirror. After that, the Slave MEMS mirror runs in a robust manner, synchronous to the Master MEMS mirror.

TABLE I

MEASUREMENT RESULTS

	Begin [1]	End [1]	t [ms]	$f_S start$ [Hz]	$f_S top$ [Hz]
Master	-	-	-	4489	4489
Slave	44715	45749	~ 110	4621	4489

V. CONCLUSION

In our paper, we have introduced a novel synchronisation procedure for MEMS-based LiDAR systems. The approach from Strasser et al. [14] is not robust and, therefore, not an option for highly automated vehicles. The novel procedure reduces the synchronisation time on the one hand and ensures a robust and reliable synchronisation of a Slave MEMS mirror to a Master MEMS mirror on the other. This means that the first research question can be answered with yes. It is possible that the FoV can be extended by synchronisation and at the same time, a robust operation can be ensured. Due to the fact that the adapted architecture can also be used for Master systems, the second research question can also be answered. No, it is not necessary to build different architectures for Master and Slave. By adaptions, it is possible to operate it either as a Master or as a Slave. Thus, our procedure can be a key enabler for robust, long-range, and wide FoV solutions in automotive applications. For highly automated vehicles, it is indispensable to have robust and reliable components and subsystems in environmental perception systems. With a wider and deeper FoV, the LiDAR part of the environmental perception system is able to detect obstacles earlier and initiate appropriate measures. This is a further step towards achieving the overall objective of protecting passengers and other traffic participants.

ACKNOWLEDGMENT

The authors would like to thank all national funding authorities and the ECSEL Joint Undertaking, which funded the PRYSTINE project under the grant agreement number 783190.

PRYSTINE is funded by the Austrian Federal Ministry of Transport, Innovation and Technology (BMVIT) under the program ICT of the Future between May 2018 and April 2021 (grant number 865310). More information: https://iktderzukunft.at/en/.

REFERENCES

[1] M. Houtenbos, H. Jagtman, M. Hagenzieker, P. Wieringa, and A. Hale, "Understanding road users' expectations: an essential step for ADAS development," *European journal of transport and infrastructure research EJTIR, 5 (4)*, 2005.

[2] L. Briesemeister, L. Schafers, and G. Hommel, "Disseminating messages among highly mobile hosts based on inter-vehicle communication," in *Proceedings of the IEEE Intelligent Vehicles Symposium 2000 (Cat. No.00TH8511)*, Oct 2000, pp. 522–527.

[3] S. Chen, J. Hu, Y. Shi, Y. Peng, J. Fang, R. Zhao, and L. Zhao, "Vehicle-to-Everything (v2x) Services Supported by LTE-Based Systems and 5G," *IEEE Communications Standards Magazine*, vol. 1, no. 2, pp. 70–76, 2017.

[4] N. Druml, G. Macher, M. Stolz, E. Armengaud, D. Watzenig, C. Steger, T. Herndl, A. Eckel, A. Ryabokon, A. Hoess, S. Kumar, G. Dimitrakopoulos, and H. Roedig, "PRYSTINE - PRogrammable sYSTems for INtelligence in AutomobilEs," in *2018 21st Euromicro Conference on Digital System Design (DSD)*, Aug 2018, pp. 618–626.

[5] SAE, "SAE International Standard J3016 - Taxonomy and Definitions for Terms Related to On-Road Motor Vehicle Automated Driving Systems," SAE International, Standard, January 2014.

[6] A. Kohn, R. Schneider, A. Vilela, A. Roger, and U. Dannebaum, "Architectural Concepts for Fail-Operational Automotive Systems," in *SAE 2016 World Congress and Exhibition*. SAE International, April 2016.

[7] H. W. Yoo, N. Druml, D. Brunner, C. Schwarzl, T. Thurner, M. Hennecke, and G. Schitter, "MEMS-based lidar for autonomous driving," *e & i Elektrotechnik und Informationstechnik*, vol. 135, no. 6, pp. 408–415, Oct 2018.

[8] M. Baumgart, C. Consani, M. Dielacher, and N. Druml, "Optical simulation of Time-of-Flight sensor accuracy in rain," in *The European Conference on Lasers and Electro-Optics*. Optical Society of America, 2017, p. CH_P_25.

[9] Velodyne LiDAR, "HDL-64E," 2016.

[10] N. Druml, I. Maksymova, T. Thurner, D. Van Lierop, M. Hennecke, and A. Foroutan, "1D MEMS Micro-Scanning LiDAR," in *The Ninth International Conference on Sensor Device Technologies and Applications (SENSORDEVICES 2018)*, 09 2018.

[11] Infineon Technologies AG. (2018) AURIX System Safety Controller. https://iot-automotive.news/aurix-microcontroller-tc3xx-family-infineon-fuels-automated-driving-electromobility.

[12] B. Borovic, A. Q. Liu, D. Popa, H. Cai, and F. L. Lewis, "Open-loop versus closed-loop control of MEMS devices: choices and issues," *Journal of Micromechanics and Microengineering*, vol. 15, no. 10, p. 1917, 2005.

[13] P. Stelzer, A. Strasser, C. Steger, A. Garcia, and N. Druml, "Fast Angle Adaption of a MEMS-based LiDAR System," *IFAC-PapersOnLine*, vol. 52, no. 15, pp. 55 – 60, 2019, 8th IFAC Symposium on Mechatronic Systems MECHATRONICS 2019.

[14] A. Strasser, P. Stelzer, C. Steger, and N. Druml, "Towards Synchronous Mode of Multiple Independently Controlled MEMS Mirrors," *IFAC-PapersOnLine*, vol. 52, no. 15, pp. 31 – 36, 2019, 8th IFAC Symposium on Mechatronic Systems MECHATRONICS 2019.

[15] G.-C. Hsieh and J. C. Hung, "Phase-locked loop techniques. A survey," *IEEE Transactions on industrial electronics*, vol. 43, no. 6, pp. 609–615, 1996.

[16] A. Strasser, P. Stelzer, C. Steger, and N. Druml, "Speed-Up of MEMS Mirror's Transient Start-Up Procedure," March 2019, 2019 IEEE Sensors Applications Symposium, SAS ; Conference date: 11-03-2019 Through 13-03-2019.